Propulsion and Power Research

Original article

Numerical simulations of cellular detonation diffraction in a stable gaseous mixture

Jian Li[a], **Jian Guo Ning**[a], **Charles B. Kiyanda**[b] and **Hoi Dick Ng**[b]

[a]*Beijing Institute of Technology, State Key Laboratory of Explosion Science & Technology, Beijing, 100081, China*
[b]*Department of Mechanical and Industrial Engineering, Concordia University, Montréal, QC, H3G 1M8, Canada*

Abstract: In this paper, the diffraction phenomenon of gaseous cellular detonations emerging from a confined tube into a sudden open space is simulated using the reactive Euler equations with a two-step Arrhenius chemistry model. Both two-dimensional and axisymmetric configurations are used for modeling cylindrical and spherical expansions, respectively. The chemical parameters are chosen for a stable gaseous explosive mixture in which the cellular detonation structure is highly regular. Adaptive mesh refinement (AMR) is used to resolve the detonation wave structure and its evolution during the transmission. The numerical results show that the critical channel width and critical diameter over the detonation cell size are about 13 ± 1 and 25 ± 1, respectively. These numerical findings are comparable with the experimental observation and confirm again that the critical channel width and critical diameter differ essentially by a factor close to 2, equal to the geometrical scaling based on front curvature theory. Unlike unstable mixtures where instabilities manifested in the detonation front structure play a significant role during the transmission, the present numerical results and the observed geometrical scaling provide again evidence that the failure of detonation diffraction in stable mixtures with a regular detonation cellular pattern is dominantly caused by the global curvature due to the wave divergence resulting in the global decoupling of the reaction zone with the expanding shock front.

Keywords: Detonations; Diffraction; Pulse detonation engine; Stable mixture; Adaptive mesh refinement
PACS: 47.40.-x, 47.40-Rs, 47.40.Nm

1. Introduction

When a gaseous detonation wave emerges from a confined geometry, either a channel or a circular tube, into an open area filled with the same reactive mixture, the detonation will fail if the channel width or tube diameter is less than some critical value [1, 2]. This phenomenon has long been a well-defined fundamental problem in understanding both initiation and failure of detonation waves. Knowledge of the critical geometrical dimension also has practical applications such as in the design of initiators for pulse detonation engines (PDE), e.g., when the detonation transmits from the small pre-detonator to the main thrust tube of the pulse detonation engine [3-7]. At specific initial conditions, these critical parameters have rather unique values for a given detonable mixture and can thus be considered as an alternative length scale that provides an assessment of the relative detonation sensitivity of a combustible mixture.

For common fuel-air mixtures which are typically unstable with an irregular detonation front structure embedded with small scale instabilities, the universal relationship for the critical tube diameter d_c has been well established to be $d_c = 13\lambda$ where λ is the characteristic detonation cell size [8-10]. Critical widths, w_c, for the successful transformation of a planar to a cylindrical detonation are also measured in a number of experiments using a thin annular or rectangular channel and show that w_c/λ is roughly about 3 [11, 12]. However, in very special mixtures such as those with high argon dilution (e.g., acetylene-oxygen mixtures with argon dilution above 70% well within the detonation limit), the aforementioned empirical correlations become invalid and experiments have shown that the scaling can be up to $d_c \sim 25\lambda$ and w_c/λ as much as 12 [11, 13-15]. In highly argon diluted mixtures, the cellular detonation structure is very regular or appears to be piece-wise laminar and, hence, it has long been suggested that the detonation stability or cell structure regularity plays an important role in the detonation undergoing a sudden expansion into open space and leads to the breakdown in the scaling between stable and unstable mixtures. Lee [16]

*Corresponding author: H.D. Ng, Telephone: 1- (514) 848-2424 (ext. 3177), E-mail: hoing@encs.concordia.ca

Peer review under responsibility of National Laboratory for Aeronautics and Astronautics.

proposed two mechanisms, one local and one global for the diffracted wave to explain the phenomenon and the difference in the λ scaling between stable and unstable mixtures. For common fuel-air, unstable mixtures, the phenomenon is characterized by the re-initiation of local explosion centers, that is linked to the effect of instabilities. For stable mixtures where the cellular structure is very regular and instability plays a less important role (e.g., explosive mixtures such as acetylene-oxygen with high percentage of argon dilution), Lee argues that the failure occurs due to the global mechanism, like an ideal ZND detonation, where the curvature of the attenuated detonation exceeds some critical value required for self-sustained propagation [17].

Although a number of numerical studies on the detonation diffraction can be found in the literature, e.g., [18-22] for gaseous mixtures as well as [23-25] for multiphase explosives, very few focus on Lee's conjecture, to discriminate between the two failure mechanisms in unstable and stable mixtures. The λ scaling observed from experiments has not yet been recovered numerically due to several limitations. A number of studies have been restricted only to two-dimensional (channel) configuration, low grid resolution, simplified one-step Arrhenius chemical kinetics, and the diffraction of an initial planar ZND detonation. In this study, a series of high resolution, numerical simulations using the two-dimensional (channel) and axisymmetric (tube), reactive Euler equations with a two-step reaction model are performed to investigate the evolution of the cellular detonation wave expanded from a small channel or tube to a larger open space in a stable mixture with highly regular cellular pattern. While it is difficult to simulate with confidence detonation waves in unstable mixtures due to the necessity to resolve various sources of instability inside the structure, for stable mixtures a sufficient level of numerical resolution can be achieved presently using adaptive mesh refinement to correctly capture the regular detonation structure and its evolution. The objectives of this work are two-folds. The numerical simulations provide the flow field during the diffraction phenomenon and confirm the critical thickness and tube diameter correlations with cell size for stable mixtures. The numerical values of w_c/λ and d_c/λ obtained from both two-dimensional and axisymmetric computations are compared to the predictions of failure mechanisms proposed by Lee [16]. If the mechanism of failure for stable detonations is based on curvature, as suggested by Lee, this should result in a 2:1 relationship between d_c and w_c. The curvature of a cylindrical surface is half that of a spherical one, as curvature in one direction does not exist, therefore the theory expects $w_c \approx d_c/2$, a geometrical factor of two. It is worth mentioning that this geometrical relation was also suggested previously through the analysis of a series of experimental data by Vasil'ev [26].

2. Problem formulation and numerical details

The present simulation of gaseous cellular detonation diffraction is based on the inviscid, reactive Euler equations for either a two-dimensional (**Z** = 0) or axisymmetric flow in channel or circular tube, respectively. Written in conserved form, these equations are represented by:

$$\frac{\partial \mathbf{U}}{\partial t}+\frac{\partial \mathbf{F}}{\partial x}+\frac{\partial \mathbf{G}}{\partial r}+\frac{\mathbf{Z}}{r}=\mathbf{S}$$

where the conservative state vector **U** and the flux vectors **F**, **G**, **Z** and the source term **S** are given by:

$$\mathbf{U}=\begin{pmatrix}\rho\\ \rho u\\ \rho v\\ E\\ \rho y_1\\ \rho y_2\end{pmatrix},\quad \mathbf{F}=\begin{pmatrix}\rho u\\ \rho u^2+p\\ \rho uv\\ u(E+p)\\ \rho u y_1\\ \rho u y_2\end{pmatrix},\quad \mathbf{G}=\begin{pmatrix}\rho v\\ \rho uv\\ \rho v^2+p\\ v(E+p)\\ \rho v y_1\\ \rho v y_2\end{pmatrix}$$

$$\mathbf{Z}=\begin{pmatrix}\rho v\\ \rho uv\\ \rho v^2\\ v(E+p)\\ \rho v y_1\\ \rho v y_2\end{pmatrix},\quad \mathbf{S}=\begin{pmatrix}0\\ 0\\ 0\\ 0\\ \dot{\omega}_1\\ \dot{\omega}_2\end{pmatrix}$$

Unless specified, all the flow variables have been made dimensionless by reference to the uniform, unburned state. The mixture is assumed to be ideal and calorically perfect with constant specific heat ratio γ. The conservation laws are coupled with a two-step chain-branching type reaction model [27, 28]. The first step represents a thermally neutral induction zone, with a temperature-sensitive Arrhenius form of the reaction rate given by:

$$\dot{\omega}_I=H(1-y_1)\rho k_I \exp\left(E_I\left(\frac{1}{T_s}-\frac{1}{T}\right)\right)$$

where k_I, E_I and T_s are the pre-exponential constant, activation energy of the induction process and shock temperature, respectively. y_1 is the progress variable of the induction process and $H(\,)$ is a step function which can be defined as:

$$H(1-y_1)=\begin{cases}1 \text{ if } y_1<1\\ 0 \text{ if } y_1\geq 1\end{cases}$$

Here, the reference length scale x_{ref} is chosen such that the one-dimensional steady ZND detonation induction length is unity, i.e., $\Delta_I = 1$. At the end of induction zone, the second step describes the rapid energy release after the branched-chain

thermal explosion and the slow heat release in the radical recombination stage. The reaction rate for this step is given by:

$$\dot{\omega}_R = \left(1 - H(1 - y_1)\right)\rho k_R (1 - y_2)\exp\left(\frac{-E_R}{T}\right)$$

where k_R and E_R denote the pre-exponential constant and activation energy for the heat release process. y_2 represents the chemical reaction progress variable. Similar to previous studies [27, 28], the reaction rate constant k_R is used as a bifurcation parameter to control the ratio of the reaction length to the induction length and, hence, the stability of the detonation wave. For ease of representation, alternative dimensionless activation energies are also introduced:

$$\varepsilon_I = \frac{E_I}{\delta}, \quad \varepsilon_R = \frac{E_R}{\delta}$$

where δ denotes the temperature jump across the leading shock. Therefore, ε is simply the reduced activation energy normalized by the temperature behind the leading shock of the ZND detonation. Here, $\varepsilon_I = 4.8$, $\varepsilon_R = 1.0$, $\gamma = 1.44$, $Q = 19.7$ and $M_{CJ} = 5.6$ are used. For a stable mixture, the pre-exponential constants of the rate laws are chosen respectively $k_I = 0.139$ and $k_R = 0.2$. The chemical parameters are chosen to represent closely a mixture of $C_2H_2 + 2.5\ O_2 + 14$ Ar, at 295 K and 50 kPa and such mixture conditions give a stable detonation with a regular cellular pattern [27, 29]. It is worth reminding that from experimental observations, in general, a stable detonation is referred to the case where cellular patterns are highly regular. As shown later in Fig. 1, the cellular pattern obtained from the numerical simulations is regularly spaced and closely resembles those observed experimentally for highly argon diluted mixtures (e.g., acetylene-oxygen with more than 70% argon dilution well within the detonation limit), as well as those obtained numerically with moderately low activation energy or stability parameter [30, 31]. Therefore, the mixture parameters chosen are well suited for the conditions to give a stable detonation with a highly regular structure.

The governing equations are then solved using the parallel AMROC code built with block-structured adaptive mesh refinement (AMR) [32]. The entire computational domain was first covered by coarse grids, and fine meshes were superimposed on the coarse grids in the vicinity of the front. A fractional steps method was used to decouple the hydrodynamic transport and chemical reaction numerically. The Euler equations are solved with an explicit second-order Godunov type numerical scheme incorporating a hybrid Roe-solver-based method. Slip wall conditions are imposed on solid boundaries. Inlet and outlet boundary conditions are imposed on the left and right boundaries, respectively. The cellular detonation and its cell size is obtained and examined a priori in a long, straight channel/tube. A fully developed, stable, cellular detonation is then mapped into the present computational domain as initial condition for the simulation of the diffraction phenomenon, (at least one cell length from the left boundary in the channel/tube). In this work, a maximum resolution of 32 points per Δ_I with four levels of Cartesian mesh adaptation with refinement factors (2, 2, 2, 4) is used.

3. Results and discussion

The diffraction process is illustrated here using both temperature contour plots and the "numerical smoked foil" showing the time-integrated maximum pressure contour from the numerical simulation, and hence the trajectories of the triple points. It is important to note that only half of the channel is considered for the computation and hence, the smoked foil figure includes also the mirror image to have the complete channel size. Figure 1 first shows the results obtained for the detonation wave exiting a two-dimensional channel (without axisymmetric consideration). Different channel widths are considered to vary the number of cells initially presented in the channel before the emergence into the larger space. The case where detonation failure occurs is shown in Fig. 1a where the channel width (or the number of cells) is below the critical value. The failure wave from the corner enters into the central axis and the resulting large curvature of the diffracting wave causes the continuous decoupling of the reaction zone from the diverging shock front. The failure is also indicated by the disappearance of the cellular pattern.

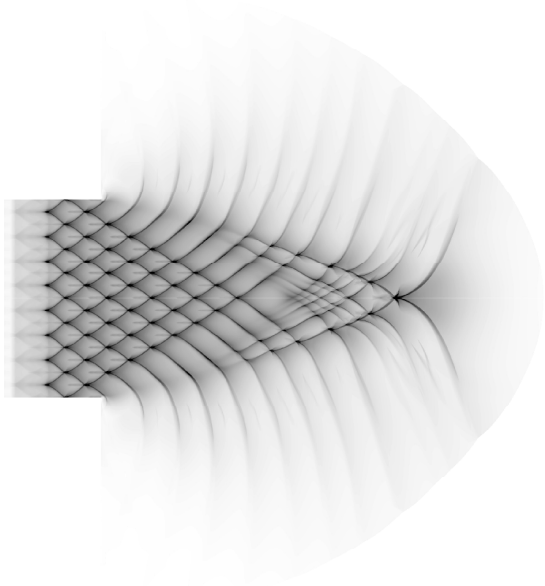

(a)

Figure 1 (continued)

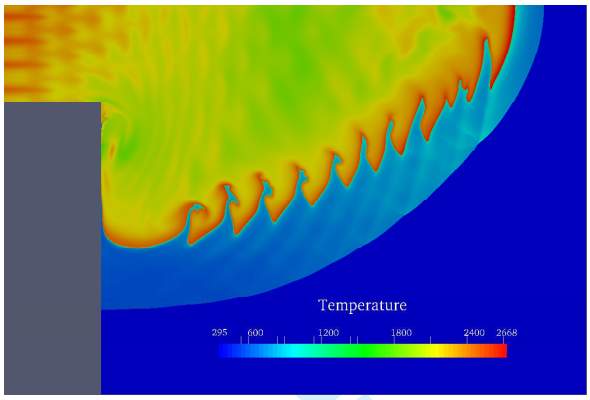

(b)

Figure 1 a) Numerical smoked foil; and b) temperature contour plot showing an unsuccessful transmission of the stable cellular detonation with initially 8 detonation cells in the channel.

Figure 2 shows the cases approaching the critical condition with an increase of the channel width to accommodate 12 and 14 detonation cells. It is found that the critical value w_c/λ is approximately 13 ± 1 which is close to the experimental result. For the successful transmission shown in Fig. 2b with initially 14 cells, the rarefaction waves first cause an enlargement of cells at the diffracting front. Nevertheless the cellular structure re-establishes globally at further distance once the effect of curvature becomes less severe. The sequence of temperature contour plots shown in Fig. 3 also indicate the transmission is a global event showing the continuous re-coupling of the reaction zone with the whole leading diverging front near the channel axis and continuous evolution of the cellular structure. This is different from the mechanism observed in unstable mixtures where re-establishment of the detonation originates from a local hot spot and randomly in any location behind the diverging front where instabilities manifest.

Another interesting feature as previously observed and discussed by Arienti and Shepherd [21] on the diffraction of a planar ZND detonation is the formation of a fold or kink in the diverging shock front which propagates toward the corner wall. This folding results from the interplay of transverse rarefaction waves with the accelerating detonation front near the channel central axis. Although this characteristic feature may appear to be the driving force for the re-initiation, it is important to note that new transverse waves must be generated to keep the average spacing (cell size) the same as the surface area of the diverging front increases. If transverse waves are not generated, the cylindrically diverging detonation still fails as it continues to expand.

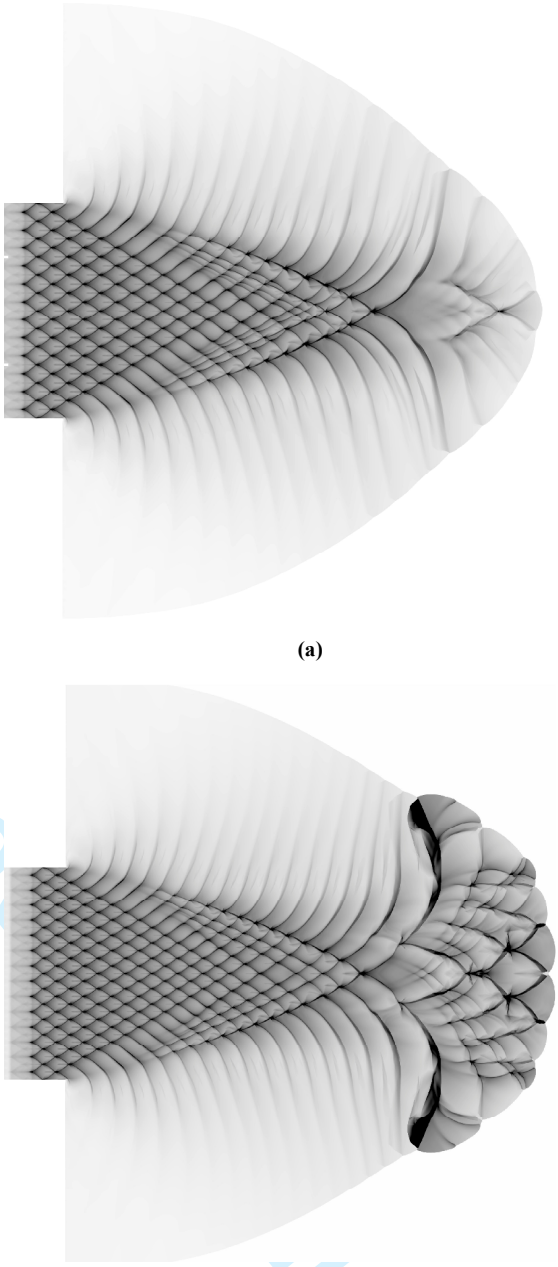

(a)

(b)

Figure 2 Numerical smoked foil for cases with initially a) 12; and b) 14 detonation cells in the channel.

Figure 4 illustrates now the results obtained for the circular tube configuration (including the axisymmetric term in the computation) with initially 24 and 26 cells in the confined region. By introducing axial symmetry and, hence, an additional curvature direction, the detonation wave emerging from the confined tube is more prompt to failure. More cells initially in the tube diameter are thus required. For successful transmission from a circular tube to an unconfined space, the present numerical results show that the number of cells

required is close to 25 ± 1, i.e., $d_c/\lambda \sim 25–26$, which is in very good agreement with the experimental observations for detonations in stable mixtures where the cell patterns are highly regular. It is perhaps worth pointing out that in the axisymmetric calculations the annular transverse waves which can reflect and provide amplification of peak pressure and some change in the cell size [25], are not traced. However, these transverse waves in highly stable mixtures are weak and their role is not as prominent as in typical unstable mixtures. Therefore, the lack of these transverse waves, as compared to the frontal curvature, should not affect much the critical values for successful transmission. Nevertheless, it is desirable in the future to carry out true 3-dimensional simulations to include the presence of these annular transverse waves as well.

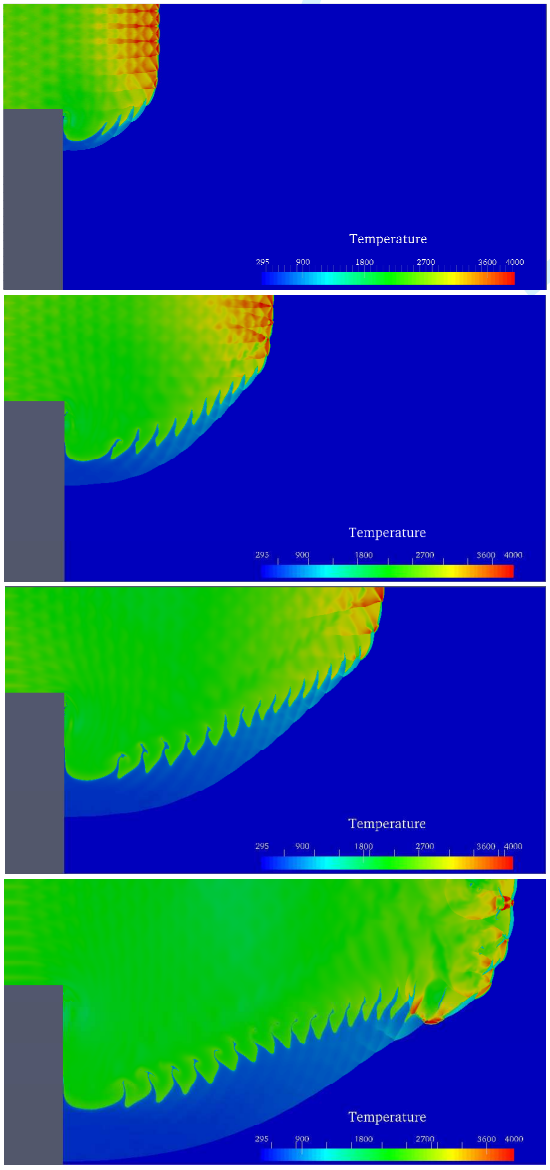

Figure 3 A sequence of temperature contour plots for the case with initially 14 detonation cells in the channel.

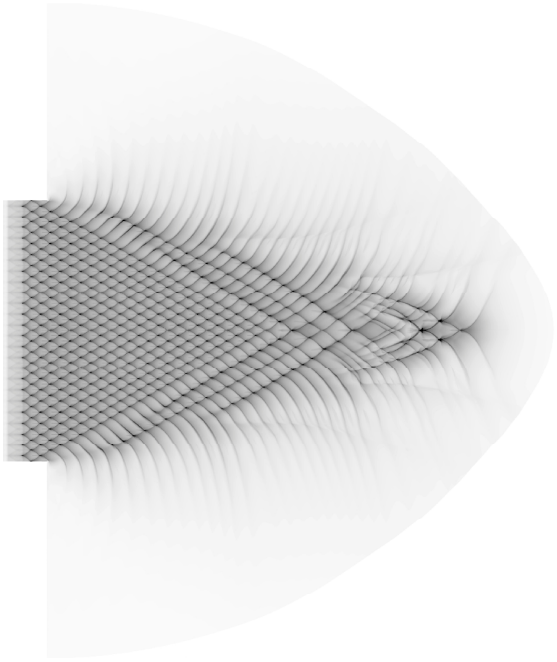

(a)

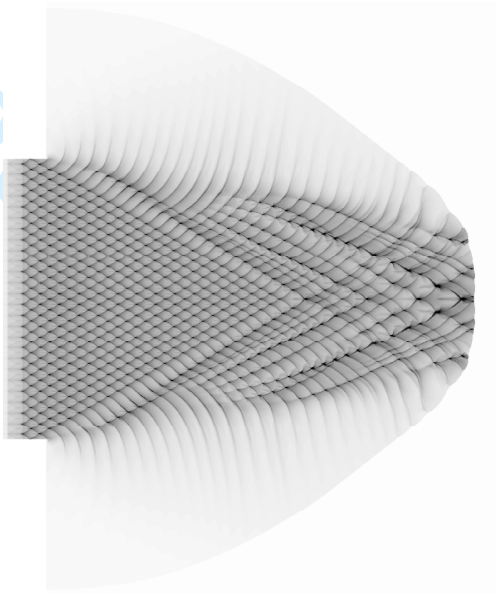

(b)

Figure 4 Numerical smoked foil for cases with initially a) 24; and b) 26 detonation cells in the confined tube.

Comparison between different scalings obtained from the present numerical simulation and available experimental data [11-15] shows rather good agreement despite the model simplification used for the computation. The numerical results of w_c/λ and d_c/λ required for the detonation to re-initiate and continue to propagate in the unconfined volume are 13 ± 1 and 25 ± 1, respectively. These results provide some important observations on the failure mechanism proposed by Lee for the

detonation diffraction phenomenon. For the stable mixture with regular cellular pattern, the present results give a ratio of d_c/w_c roughly equal to a factor of 2, corresponding to the geometrical factor of the curvature term between a spherical and cylindrical diverging wave. In other words, from geometrical considerations based on front curvature theory, one would expect the critical diameter to be twice the critical channel width. Hence, the current numerical simulations provide evidence to a failure mechanism based on curvature, given that this ratio of critical diameter to critical width near 2 arises for the stable mixture.

4. Conclusion

In this study, a numerical investigation is carried out on the problem of detonation diffraction in a stable gaseous mixture, where it has been suggested that the cellular instabilities play a minor role in the detonation propagation mechanism. The failure results from a continuous enlargement and subsequent disappearance of cells and the deceleration of the diverging wave due to curvature leads to the decoupling of the reaction zone with the leading front. For the successful transmission, the cellular structure survives and re-establishes at a further distance. It relies on the ability to maintain a global coupling between the diverging shock front and the reaction zone. Consistent with previous studies on the detonation diffraction phenomenon, a characteristic feature of shock folding or kink in the diverging shock front propagating toward the corner wall is also observed to stimulate the re-coupling between the reaction zone and the leading front for re-initiation.

The present numerical results provide some important confirmation on the failure mechanisms proposed by Lee for a detonation emerging from a confined space into an open area. By comparing the critical channel width for diffracted detonations to that of the critical diameter, a factor near 2 arose for the mixture that is highly stable with regular cellular structure. Again, this result appears to support a curvature based mechanism for diffraction failure in stable detonations where the scaling of critical values d_c/w_c for the same mixture parameters (hence same cell size λ) is 2, corresponding to the geometrical factor of the curvature term between a spherical and cylindrical diverging wave. In other words, geometric considerations predict that for the same mixture conditions the scaled critical channel width w_c/λ should be half the scaled critical diameter d_c/λ because a detonation in a channel has curvature in only one plane while a detonation in a circular tube has curvature in two orthogonal planes. Hence, two times more cells at the front are needed for a stable detonation wave emerging from a tube than from a channel for the diverging detonation to successfully transmit into open space. At last, it is worth noting that these numerical results as well as the observed geometrical scaling are consistent with previous findings [11, 33-35], which all show that the global curvature is the dominant mechanism for the gaseous detonation failure and detonation instabilities do not play a prominent role on the transmission.

Acknowledgements

This work is supported by the Natural Sciences and Engineering Research Council of Canada (NSERC) and National Natural Science Foundation of China (No. 11390363, No. 11325209).

References

[1] J.H.S. Lee, The Detonation Phenomenon, New York, Cambridge University Press, 2008.

[2] A.A. Vasil'ev, Dynamic parameters of detonation, in: F. Zhang (Ed.), Shock Waves Science and Technology Library, Vol 6: Detonation Dynamics, Springer, Berlin Heidelberg, 2012, Chap. 4.

[3] S. Eidelman and W. Grossmann, Pulse detonation engine: experimental and theoretical review, 30th AIAA Aerospace Science Meeting, Reno, NV, January 6-9, 1992, AIAA paper No. 92-3168.

[4] T. Bussing and G. Pappas, An introduction to pulse detonation engines, 32nd AIAA Aerospace Science Meeting, Reno, NV, January, 10–13, 1994, AIAA paper No. 94-0263.

[5] K. Kailasanath, Recent developments in the research on pulse detonation engines, AIAA Journal 41 (2) (2003) 145-159.

[6] F.K. Lu, Prospects for detonations in propulsion, Proceedings of the 9th International Symposium on Experimental and Computational Aerothermodynamics of Internal Flows (ISAIF9), Gyeongju, Korea, September 8-11, 2009, Paper No. IL-2.

[7] G.D. Roy, S.M. Frolov, A.A. Borisov and D.W. Netzer, Pulse detonation propulsion: challenges, current status, and future perspective, Progress in Energy and Combustion Science 30 (2004) 545-672.

[8] V.V. Mitrofanov, R.I. Soloukhin, The diffraction of multifront detonation waves. Soviet Physics-Doklady 9(12) (1965) 1055.

[9] R. Knystautas, J.H. Lee, C. Guirao, The critical tube diameter for detonation failure in hydrocarbon-air mixtures. Combustion and Flame 48 (1982) 63-83.

[10] A.A. Vasil'ev, V.V. Mitrofanov, M.E. Topchian, Detonation waves in gases. Combustion, Explosion and Shock Waves 23 (1987) 605-623.

[11] J. Meredith, H.D. Ng and J.H.S. Lee, Detonation diffraction from an annular channel. Shock Waves 20 (2010) 449-455.

[12] Y.K. Liu, J.H. Lee and R. Knystautas, Effect of geometry on the transmission of detonation through an orifice. Combustion Flame 56 (1984) 215-225.

[13] D. Desbordes, C. Guerraud, L. Hamada and HN Presles, Failure of classical dynamic parameters relationships in highly regular cellular detonation systems. Progress in Astronautics and Aeronautics 153 (1993) 347-359.

[14] I. Moen, A. Sulmistras, G.O. Thomas, D. Bjerketvedt, P.A. Thibault, Influence of cellular regularity on the behavior of gaseous detonations. Progress in Astronautics and Aeronautics 106 (1986) 220-243.

[15] B. Zhang, N. Mehrjoo, H.D. Ng, J.H.S. Lee and C.H. Bai, On the dynamic detonation parameters in acetylene-oxygen mixtures with varying amount of argon dilution. Combustion and Flame 161(5) (2014) 1390-1397.

[16] J.H.S. Lee, On the critical tube diameter, in: J. Bowen (Ed.), Dynamics of Exothermicity, Gordon and Breach, Amsterdam, 1996, pp. 321.

[17] J. Yao, D.S. Stewart On the normal shock velocity-curvature relationship for materials with large activation energy. Combustion and Flame 100 (4) (1995) 519–528.

[18] C.P. Li and K. Kailasanath, Detonation transmission and transition in channels of different sizes, Proceeding of the Combustion Institute, 28 (2000) 603-609.

[19] H.Y. Fan and F.K. Lu, Numerical simulation of detonation processes in a variable cross-section chamber, Proceedings of the Institute of Mechanical Engineer Part G: Journal of Aerospace Engineering 222 (5) (2008) 673-686.

[20] D.A. Jones, G. Kemister, E.S. Oran and M. Sichel, The influence of cellular structure on detonation transmission, Shock Waves Journal 6 (1996) 119-129.

[21] M. Arienti and J.E. Shepherd, A numerical study of detonation diffraction. Journal of Fluid Mechanics 529 (2005) 117-146.

[22] M.V. Papalexandris, J.F. Thomas, C. Jacobs and V. Deledicque, Structural characteristics of detonation expansion from a small channel to a larger one, Proceeding of the Combustion Institute, 31 (2007) 2407–2414.

[23] A.V. Fedorov, T.A. Khmel, Yu V. Kratova, Shock and detonation wave diffraction at a sudden expansion in gas–particle mixtures. Shock Waves 18(4) (2008) 281-290.

[24] A.V. Fedorov, T.A. Khmel, Yu V. Kratova, Cellular detonation diffraction in gas - particle mixtures. Shock Waves 20 (6) (2010) 509-519.

[25] A. Briand, B. Veyssiere, B.A. Khasainov, Modelling of detonation cellular structure in aluminium suspensions. Shock Waves 20 (6) (2010) 521-529.

[26] A.A. Vasil'ev, Critical conditions for initiation of multifront cylindrical detonation. Combustion, Explosion and Shock Waves, 34 (1998) 220-225.

[27] H.D. Ng, M.I. Radulescu, A.J. Higgins, N. Nikiforakis and J.H.S. Lee, Numerical investigation of the instability for one-dimensional Chapman-Jouguet detonations with chain-branching kinetics, Combust. Theory Model. 9 (2005) 385-401.

[28] M. Short and G.J. Sharpe, Pulsating instability of detonation with a two-step chain-branching reaction model: theory and numerics, Combustion Theory Modelling, 7 (2003) 401–416.

[29] J. Li, J. Ning and J.H.S. Lee, Mach reflection of a ZND detonation wave. Shock Waves, 25(3) (2015) 293-304.

[30] H.D. Ng and F. Zhang, Detonation instability, in: F. Zhang (Ed.), Shock Waves Science and Technology Library, Vol 6: Detonation Dynamics, Springer, Berlin Heidelberg, 2012, Chap. 3.

[31] G.J. Sharpe and J.J. Quirk, Nonlinear cellular dynamics of the idealized detonation model: Regular cells, Combustion Theory Modelling, 12 (2008) 1-21.

[32] R. Deiterding, AMROC - Blockstructured Adaptive Mesh Refinement in Object-oriented C++, http://amroc.sourceforge.net

[33] N. Mehrjoo, B. Zhang, R. Portaro, H.D. Ng and J.H.S. Lee, Response of critical tube diameter phenomenon to small perturbations for gaseous detonations, Shock Waves Journal, 24(2) (2014) 219-229.

[34] N. Mehrjoo, R. Portaro and H.D. Ng, A technique for promoting detonation transmission from a confined tube into larger area for pulse detonation engine applications. Propulsion and Power Research. Vol. 3(1) (2014) 9-14.

[35] N. Mehrjoo, Y. Gao, C.B. Kiyanda, H.D. Ng and J.H.S. Lee, Effects of porous walled tubes on detonation transmission into unconfined space. Proceedings of the Combustion Institute 35(2) (2015) 1981-1987.